Structure/Property Relationships in Sintered and Thermally Sprayed WC-Co

S.F. Wayne and S. Sampath

Thermally sprayed WC-Co is widely used as a wear-resistant coating for a variety of applications. Although it is well established that thermal spray processes significantly affect chemistry, microstructure, and the phase distribution of WC-Co coatings, little is known about how these changes influence wear resistance. In this study, the microstructure and wear behavior of sintered and thermally sprayed WC-Co materials are examined. Powders of WC-12 wt% Co and WC-17 wt% Co were pressed and sintered, as well as thermally sprayed by high-velocity oxy-fuel (HVOF), air plasma spray (APS), and vacuum plasma spray (VPS) techniques. Results indicated considerable differences in the resulting microstructures, mechanical properties, and wear resistance. The thermally sprayed coatings showed anisotropic fracture toughness, whereas the sintered materials did not. It was also shown that a combined mechanical property/microstructure parameter, based on considerations of indentation fracture mechanisms, can be used in most cases to describe abrasive and erosive wear resistance of thermally sprayed WC-Co materials as follows:

$$\text{Wear resistance } \alpha \left(K_{IC}^{3/8} H^{1/2}\right)\left(\frac{V_f^{Co}}{1 - V_f^{Co}}\right)$$

where K_{IC} is the indentation fracture toughness, H is hardness, and V_f^{Co} is the volume fraction of cobalt. This relationship provides a means for assessing wear resistance of WC-Co coatings intended for industrial applications requiring abrasion and/or erosion resistance.

1. Introduction

THE characteristic high hardness and wear resistance of thermally sprayed WC-Co materials have made them the material of choice for use as protective coatings in a variety of industrial applications. These cermets combine the hard, brittle WC and ductile Co phases in various proportions and grain sizes to produce materials with a wide range of physical properties. It is well established that, for sintered cemented carbide materials, the cobalt content and WC grain size *in combination* control strength, hardness, and fracture toughness.[1-3] Similar observations have been made regarding thermally sprayed WC-Co coatings.[4,5]

The microstructure of thermally sprayed WC-Co is strongly dependent on powder characteristics and processing conditions.[6-8] Thermal spray conditions and spray environment (inert, low pressure, etc.) affect the extent of decarburization, degree of melting, and therefore the microstructural characteristics of the coating and its performance. Considerable variations in porosity, carbide content, and mean free path of binder arise due to differences in powder particle size, starting carbide size, and method of powder manufacture. Many researchers attribute variations in physical properties of thermally sprayed WC-Co to the decarburization of WC through an oxidation process.[6,8-11] The work of Rangaswamy and Herman[12] has underscored the importance of microstructure in determining the wear properties of thermally sprayed WC-Co coatings. These authors identified WC grain size, mean free path of cobalt, porosity, and carbon content as important microstructural parameters that influence the physical properties and performance of WC-Co coatings. They have further shown that, in the case of plasma-sprayed coatings, higher carbon content, lower mean free path, and denser coatings offer superior resistance to abrasion and particle erosion.[12]

Recent developments in high-velocity oxy-fuel flame spraying (HVOF) have enabled the production of coatings with minimal porosity and decarburization.[4,5,13,14] Nerz *et al.*[4,13] have compared the microstructures of HVOF, high-energy plasma, and conventional plasma-sprayed WC-12 wt% Co coatings. They concluded that the plasma-sprayed coatings show a larger degree of decarburization compared to the HVOF coatings. This further translated into lower abrasion resistance.

Several studies have examined the relationship between feedstock powder characteristics, process condition, and wear resistance of thermally sprayed WC-Co coatings.[6,7] It has been shown that hardness[15] and abrasion resistance[7] can be related to the microstructure of thermally sprayed WC-Co. Early attempts to correlate hardness and scratch test measurements on WC-Co coatings were unsuccessful and led to the conclusion that these techniques could not be used as a basis for developing a universal criterion for wear resistance.[16] Abrasive and erosive wear processes involve material removal by fracture and/or plastic flow associated with surface penetration and cutting action by hard particles.[17] Recent work has shown that the abrasion and erosion resistance of sintered WC-Co materials can be correlated to a combined microstructure/mechanical property relationship, which accounts for the WC grain size, cobalt content, and binder mean free path.[18,19] Because the microstruc-

Key Words: abrasion, erosion, hardness, indentation fracture toughness, WC-Co, wear

S.F. Wayne, GTE Laboratories Incorporated, Waltham, Massachusetts, and **S. Sampath,** GTE Products Corporation, Chemical and Metallurgical Division, Towanda, Pennsylvania.

ture of thermally sprayed WC-Co controls the fracture behavior, and that fracture describes, in part, the wear behavior, then it follows that the microstructure of WC-Co coatings should dictate the abrasion and erosion resistance. In this article, the wear resistance of sintered and thermally sprayed WC-Co materials subjected to diamond abrasion and gas-jet Al_2O_3 particle erosion are examined and the applicability of a combined microstructural/mechanical property relationship is assessed as a means of predicting wear resistance.

2. Material Characterization and Experimental Methods

Two compositions of WC-Co thermally sprayed powders—WC-12 wt% Co and WC-17 wt% Co—were used in this study. The characteristics of the powders are listed in Table 1. Powders were thermally sprayed (parameters are listed in Tables 2 and 3) onto degreased and grit-blasted mild steel substrates to a maximum thickness of 400 μm using three thermal spray processing techniques: air plasma spraying (APS), vacuum plasma spraying (VPS), and high-velocity oxy-fuel spraying (HVOF). In addition, the same powders were cold pressed and then sintered in a hydrogen furnace at 1375 °C to obtain fully dense compacts. The materials were characterized using X-ray diffraction, optical microscopy, immersion density, hardness, and fracture toughness. The Knoop microhardness was measured on cross sections polished through 1-μm diamond paste. Fracture toughness was also determined on polished cross sections using an indentation technique that used a Vickers indentation to generate cracks from the corners of the indent.[20] The indentation fracture toughness (IFT) was then calculated using the following relationship:

$$\text{IFT} = \frac{0.113\, HD^{1/2}}{\left(1 + \frac{C_L}{2D}\right)^{3/2}} \quad [1]$$

where H is the Knoop microhardness (GPa), 10-kg load; D is the diagonal of Vickers indentation (μm); C_L is the total crack length, which equals:

$$\sum_{n=1}^{4} C_n$$

and C_n is the length of cracks emanating from each of the four corners of the Vickers indentations.

The abrasive wear tests were carried out using a block-on-disk apparatus in which the disk was covered with a resin-bonded 30-μm diamond plate. The WC-Co block surface was a square geometry (1.25 by 1.25 cm) that was tested with an applied load of 1 kg for a total of 5 min. Abraded volume loss was calculated using the weight loss measured at 1-min intervals, divided by the density. Details concerning the abrasive wear testing apparatus and testing procedures have been previously reported.[18]

The particle erosion tests conformed to ASTM-G-76 methods. In this test, a nozzle (0.9-mm diameter) is placed 1 mm from the polished WC-Co surface (90° orientation), upon which 50-μm Al_2O_3 particles are then impacted at a velocity of 115 ms^{-1} using an argon gas carrier. All tests were performed at room temperature for 15 s, corresponding to 1.6 g of Al_2O_3 abrasive being impinged on the sample without penetration to the steel substrate. The samples were then ultrasonically cleaned in methanol, and the volume of the eroded cylindrical hole was calculated from depth gauge readings and optical measurements of the diameter.

3. Results

Figure 1 compares the optical micrographs of the metallographic cross sections of WC-12 wt% Co and WC-17 wt% Co materials processed by sintering, HVOF, APS, and VPS techniques. These microstructures reveal differences in the WC grain size distribution, extent of porosity, and the presence of carbide-deficient cobalt pools. All microstructures were corroborated using scanning and backscattered electron micros-

Table 1 Powder Characteristics

Characteristic	WC-12 wt% Co	WC-17 wt% Co
W, wt%	82.4	78.4
C, wt%	5.4	4.8
Co, wt%	12.5	16.6
Average WC size, μm	1.5	4.3
Average particle size, μm	34.5	32.4

Table 2 Spray Parameters

Material	WC-12 wt% Co		WC-17 wt% Co	
Deposition technique	APS	VPS	APS	VPS
Gun (Plasma Technik)	PT F4-MB	PT F4-VB	PT F4-MB	PT F4-VB
Nozzle diameter, mm	6	7	6	7
Current (A)/voltage (V)	650/70	700/61	600/77	650/57
Argon flow, slpm	73.5	45	50	50
Helium flow, slpm	90	79	150	20
Hydrogen flow, slpm	...	...	...	3
Carrier argon flow, slpm	4.7	2	4.5	3
Chamber pressure, mbar	...	64	...	45
Spray distance, mm	100	350	130	375
Powder feed rate, g/min	30	40	40	40

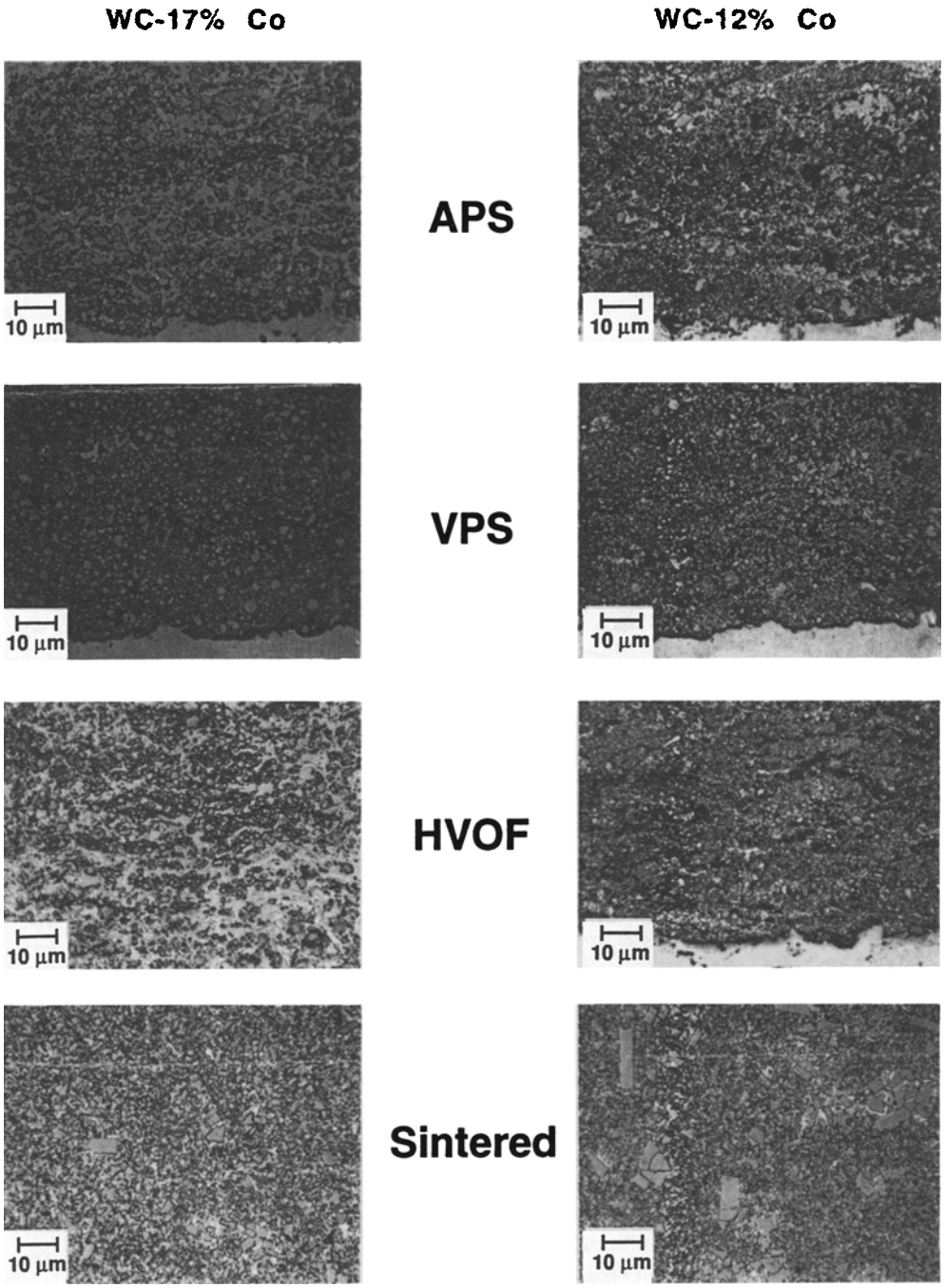

Figure 1 Light micrograph of cross-sectioned WC-Co materials.

Table 3 High-Velocity Oxy-fuel Spray Parameters

HVOF system	Jet Kote(a)
Fuel (propylene)	0.55 MPa (55% flow)
Oxygen	0.86 MPa (80% flow)
Carrier (argon)	0.45 MPa (50% flow)
Spray distance	15 cm
Feed rate	2.5% rpm

(a) Jet Kote is a trademark of Thermadyne Stellite, St. Louis, Missouri.

copy. Summarized below is a detailed interpretation of the microstructures.

3.1 *WC-12 wt% Co*

The micrographs of the WC-12 wt% Co APS and VPS coatings reveal considerable porosity. The APS coating contains partially melted particles, cobalt pools, and a predominantly fine (1 to 2 μm) carbide grain size. The VPS coating also shows poros-

Table 4 Density and Phase Analysis of Sintered and Thermally Sprayed WC-Co

Material condition	Density, g/cm^3	Phases Major	Minor
WC-12 wt% Co			
Powder	...	WC	W_2C, Co
SIntered	14.05	WC	Co
APS	13.12	W_2C, WC	W, Co
VPS	13.18	WC	W_2C, Co
HVOF	13.56	W_2C, WC	W
WC-17 wt% Co			
Powder	...	WC	Co
Sintered	13.68	WC	Co
APS	13.54	W_2C, WC	W, Co
VPS	...	WC	W_2C, W, Co
HVOF	...	W_2C, WC	W, Co

Table 5 Mechanical Properties of Sintered and Thermally Sprayed WC-Co

Material condition	Hardness(a), GPa	Indentation fracture toughness (K_{IC})(b), MPa$\sqrt{m}$ Parallel	Perpendicular
WC-12 wt% Co			
Sintered	11.9 ± 0.7	7.8 ± 1.2	7.2 ± 0.7
VPS	4.5 ± 0.7	1.2 ± 0.2	5.1 ± 0.8(c)
APS	7.9 ± 0.9	1.6 ± 0.5	9.7 ± 2.7
HVOF	9.8 ± 0.8	1.1 ± 0.2	11.1 ± 1.2
WC-17 wt% Co			
Sintered	10.6 ± 0.2	9.5 ± 0.5	9.6 ± 0.9
VPS	10.1 ± 0.5	4.1 ± 0.5	11.3 ± 2.3(c)
APS	9.4 ± 0.9	1.5 ± 0.4	13.5 ± 1.4
HVOF	10.4 ± 0.2	0.9 ± 0.2	9.7 ± 2.3(c)

(a) Hardness number, 300-g Knoop ($n = 5, \bar{x} = \pm r$) (r = 1 standard deviation). (b) Indentation fracture toughness ($n = 5, \bar{x} = \pm r$) parallel and perpendicular refer to surface plane of substrate, 10-kg Vickers load. (c) Vickers load reduced to 5 kg.

ity; however, the pores are smaller in dimension compared to the APS coating. The carbide distribution is uniform, with no evidence of cobalt pools. The immersion densities of WC-12 wt% Co APS and VPS coatings are similar (Table 4), suggesting that some of the large porosity observed in the APS coating micrograph may have resulted from polishing. The HVOF coating has a higher immersion density and a uniform, fine carbide distribution in the deposit (Fig. 1). The sintered material shows a wide variation in carbide grain size with no apparent porosity. The larger carbide grains are due to coarsening that occurred during liquid phase sintering.

X-ray diffraction analysis (Table 4) revealed considerable presence of W_2C and W phases in the APS and the HVOF coatings in addition to the WC phase. The matrix contained dissolved tungsten. Contrary to this, the VPS coating and the sintered material show little or no decomposition of the WC phase, resulting in mainly WC and Co phases in their microstructures. The larger degree of decarburization in this set of HVOF coatings may be attributed to oxidizing conditions in the flame.

3.2 *WC-17 wt% Co*

This powder contains a higher cobalt content and a larger starting average WC grain size (Table 1). The APS coating cross section, shown in Fig. 1, reveals some porosity and large pools of the matrix. The VPS coating shows a uniform carbide distribution with porosity similar to that of the APS coating. The HVOF coating cross section shows very little porosity and uniform distribution of the carbides and relatively smaller mean free path compared to the APS coating. The micrograph of WC-17 wt% Co sintered material shows no apparent porosity and a wide variation in carbide size distribution, similar to the WC-12 wt% Co sintered material. X-ray diffraction analysis (Table 4) indicated substantial presence of W_2C and W phases in the coatings, in addition to WC phase, which is similar to the observations in corresponding WC-12 wt% Co coatings.

Table 5 gives the hardness and indentation fracture toughness (K_{IC}) measurements on the coatings and the sintered compacts. There are two columns of K_{IC} data on each of the coatings. The K_{IC} parallel column refers to indentation fracture toughness values measured from cracks running parallel to the coating/substrate interface. The K_{IC} perpendicular column refers to indentation fracture toughness values measured from cracks running perpendicular to this interface. It is clear from Table 5 that the sintered materials are isotropic in fracture toughness, whereas the thermally sprayed materials show considerable anisotropy in fracture toughness. Such anisotropic physical properties of thermally sprayed coatings have been reported by Nakahira *et al.*[21] The low toughness direction is parallel to the interface and is thought to be the result of weak bonding between splats (low cohesive strength). The highest resistance to crack propagation is observed to be perpendicular to the coating/substrate interface, and these are the values that have been chosen for the correlation studies in this article.

Sintered WC-12 wt% Co materials, used for both metal cutting and mechanical seals, typically have values of fracture toughness IFT ≅ 8 MPa$\sqrt{m}$ and hardness KHN ≅ 14 GPa. The values of fracture toughness (5.1 to 13.5 MPa$\sqrt{m}$) and hardness (4.5 to 11.9 GPa) obtained on thermally sprayed coatings show that these materials possess mechanical properties approaching those of sintered WC-Co material. For reference, the Knoop microhardness of cobalt metal is ≈3 GPa, whereas binderless, dense polycrystalline WC is ≈23 GPa. As shown in Table 5, for fracture toughness measurements, the Vickers load was reduced in some cases to obtain the appropriate crack morphology. This load is accounted for in the fracture toughness calculation, and the various values can therefore be compared.

Abrasive wear resistance of the WC-Co materials is plotted in Fig. 2(a). The sintered materials show the highest resistance to abrasion, with HVOF coatings somewhat lower by comparison. The plasma-sprayed coatings (APS and VPS) show significantly lower abrasion resistance. Noteworthy is the similarity in wear performance of WC-12wt% Co and the WC-17 wt% Co coatings in light of microstructural differences.

Figure 2(b) shows the erosion resistance of the various WC-Co materials. No apparent pattern is observed on the erosion performance of the various coatings. The WC-12 wt% Co

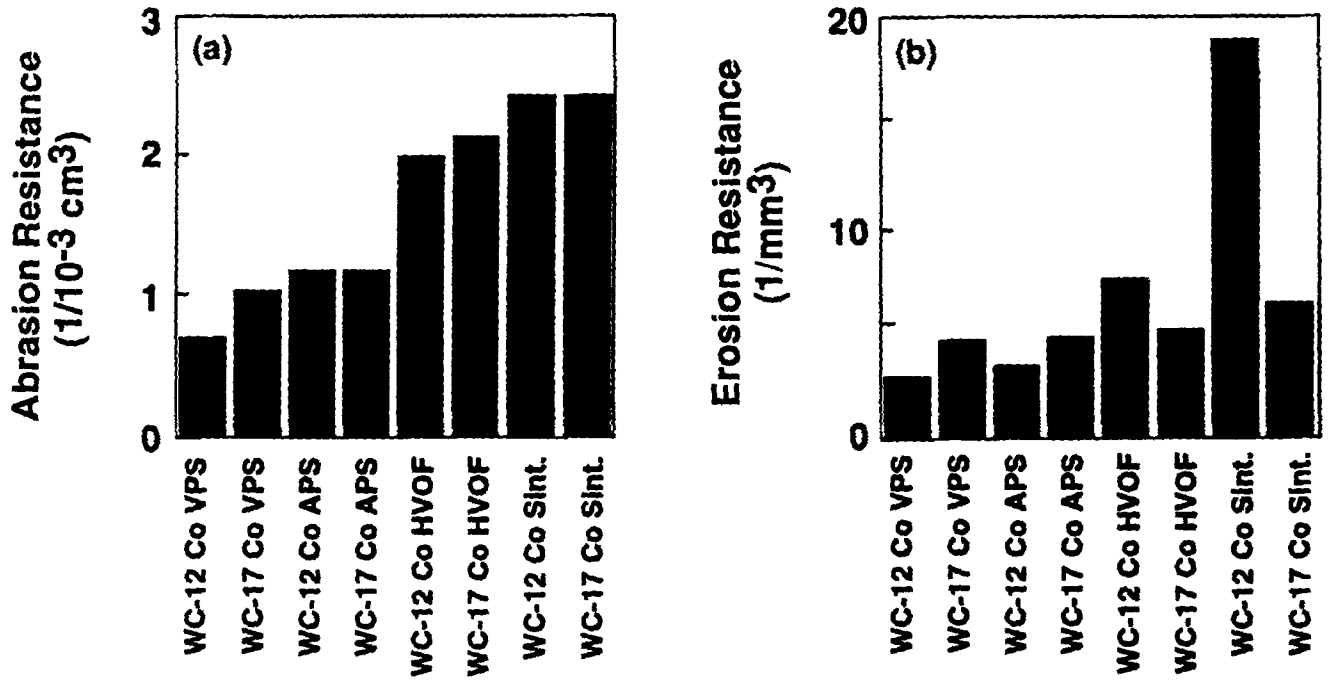

Figure 2 (**a**) Abrasive wear resistance of WC-12 wt% Co and WC-17 wt% Co. (**b**) Erosive wear resistance of WC-12 wt% Co and WC-17 wt% Co.

HVOF coating and the sintered compact show the highest erosion resistance.

4. Discussion

The physical properties of thermally sprayed WC-Co coatings are related to their complex microstructures. The key microstructural differences between the various WC-Co materials used in this study are porosity, mean free path of binder, and carbide grain diameter. Porosity plays a deleterious role in WC-Co coatings by reducing the cohesive strength, adhesive bond, and the hardness of the coating. This result is apparent when the microstructures in Fig. 1 are compared with their corresponding fracture toughness and hardness values (Table 5).

4.1 *Abrasion*

The nature of the abrasion process in WC-Co alloys clearly involves plastic deformation and fracture. It had been shown earlier[18] that the abrasive wear resistance of Si_3N_4- and Al_2O_3-based ceramics is dominated by brittle fracture and can be described by the mechanical property parameter $K_{IC}^{3/4}H^{1/2}$. In the same study, the abrasion resistance of sintered WC-6 wt% Co materials, with nearly equivalent hardness to the ceramics, was more appropriately approximated by $K_{IC}^{3/8}H^{1/2}$. In a subsequent paper, the importance of including a microstructural parameter to account for cobalt content and binder mean free path was identified as:[19]

$$\text{Wear resistance } \alpha K_{IC}^{3/8}H^{1/2}\left(\frac{\lambda}{\bar{D}_{wc}}\right) \qquad [2]$$

It is important to note that the calculation of mean free path (λ) in WC-Co materials assumes that the cobalt alloy binder surrounds each WC grain, defined as:

$$\lambda = \frac{V_f^{Co}}{1 - V_f^{Co}} \cdot \bar{D}_{wc} \qquad [3]$$

and as such is a consequence of the WC grain size ($\bar{D}_{wc}$) and the volume fraction of cobalt (V_f^{Co}). This study has shown that the abrasive and erosive wear resistance of sintered WC-Co cermets was proportional to the combined microstructure/mechanical property parameter:

$$\left(K_{IC}^{3/8}H^{1/2}\right)\left(\frac{V_f^{Co}}{1 - V_f^{Co}}\right) \qquad [4]$$

over a wide range of WC grain sizes and cobalt contents.[19]

The abrasion resistance results shown in Fig. 2(a) do not show a strong dependence on the volume fraction of cobalt. The interrelationship between the microstructure and mechanical properties of thermally sprayed WC-Co materials has as an added complexity—the differences in deposition techniques, which can alter the chemical composition of WC and cobalt binders (therefore λ) and subsequently wear resistance. In addition, the splat-type microstructures created during thermal spraying lead to anisotropic fracture toughness and further variations in wear resistance. Nevertheless, the current approach has been to correlate the resulting mechanical properties of thermally sprayed WC-Co to measured wear resistance. Figure 3(a)

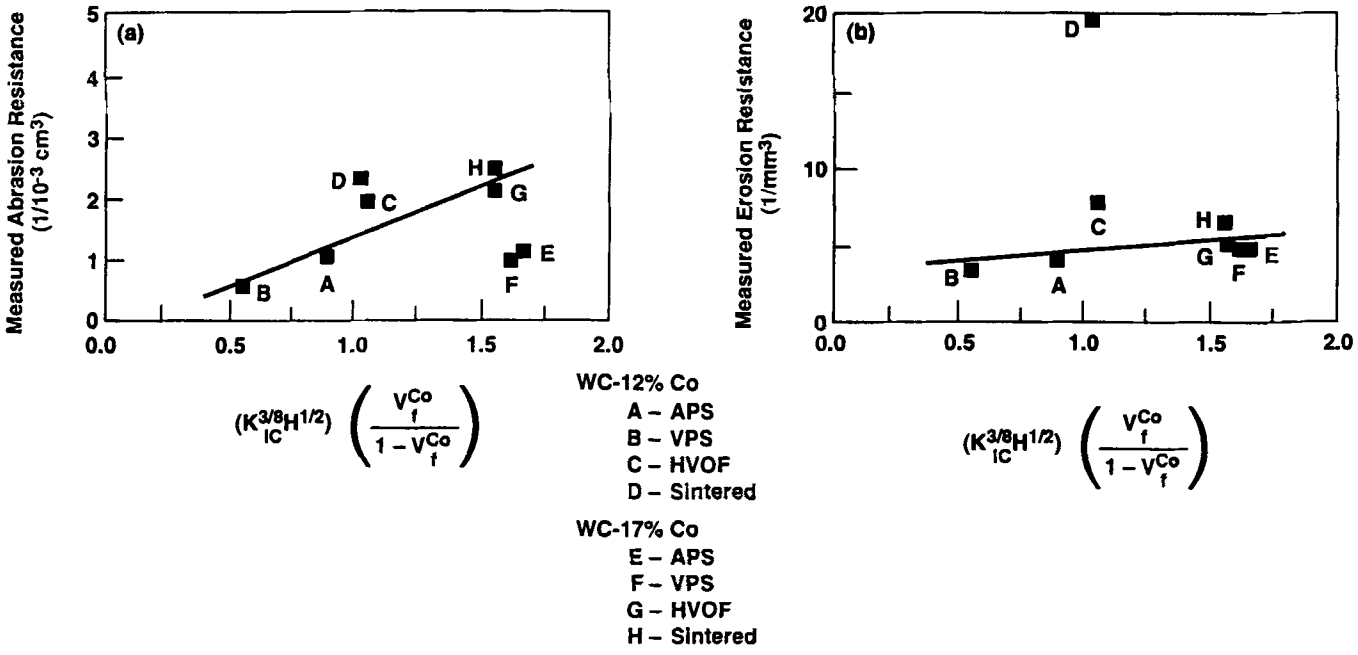

Figure 3 (a) Abrasive and (b) erosive wear resistance of WC-Co materials versus structure/property parameter.

contains a plot of abrasive wear resistance versus the structure/property parameter:

$$\left(K_{IC}^{3/8}H^{1/2}\right)\left(\frac{V_f^{Co}}{1-V_f^{Co}}\right)$$

These data show that, in spite of a wide variance in physical properties, cobalt content, WC grain size distribution, and wear resistance, an approximate correlation is obtained for sintered and thermally sprayed WC-Co materials. The WC-17 wt% Co APS and VPS coatings (coded as E and F) show considerable divergence from the abrasion parameter correlation, and it is generally believed that variations in measurements of microhardness and fracture toughness arising from microstructural inhomogeneities, carbide dissolution, and anisotropy may account for some of the observed differences.

The WC-12 wt% Co coatings have a smaller volume fraction of cobalt and a finer grain size and show equal or lower resistance to abrasion than the WC-17 wt% Co coatings. Additionally, the VPS coating has retained most of the WC phase, yet shows poor mechanical properties and abrasion resistance. Porosity appears to be the major problem in this set of VPS coatings. The origin of this porosity may be attributed to a high substrate coating system temperature during VPS deposition (>800 °C).[22] Large thermal expansion mismatch between the steel substrate and the coating (almost a factor of two) can lead to substantial residual stresses in the coating, of particular significance in the case of the low-cobalt alloy. High temperature may also cause recrystallization and phase transformations in the matrix and reduce hardness.

These results suggest that coating porosity and cohesive strength may dominate other factors such as WC grain size and cobalt content. An interesting feature of the present correlation is that both hardness and fracture toughness measurements incorporate factors such as porosity, particle/matrix bond, WC grain size, and mean free path. An attempt has been made to express the abrasion resistance of plasma-sprayed WC-Co coatings in an unambiguous, quantitative manner as a function of mechanical properties and microstructure.

4.2 *Erosion*

The erosion resistance of sintered and HVOF-sprayed WC-Co materials shows that reducing the cobalt content leads to improvements in erosion resistance (Fig. 2b). The opposite behavior, although to a lesser extent, was obtained by APS and VPS spray techniques, which contained larger porosity. These variations in wear resistance would be anticipated from the generally lower values of hardness and fracture toughness created by APS and VPS spraying (Table 5). However, it is not apparent that hardness or fracture toughness—as independent parameters—would correlate to erosion resistance. In fact, attempts to correlate hardness to wear resistance often lead to erroneous predictions. Figure 3(b) is a plot of erosion resistance versus the combined microstructure/property parameter:

$$\left(K_{IC}^{3/8}H^{1/2}\right)\left(\frac{V_f^{Co}}{1-V_f^{Co}}\right)$$

This plot, which contains results obtained on thermally sprayed WC-Co and sintered materials, shows that, in spite of significant variations in composition and thermal processing, a correlation can be obtained. The established relationship, although demonstrated to be generally valid for WC-Co materials, has been shown to provide fairly accurate predictions for sintered WC-Co materials with controlled microstructures.[19] In this prior study, it was shown that the highest erosion resistance was achieved with binderless WC and the least with pure cobalt metal. Clearly, the reduction of cobalt content in WC-Co materials, and consequently the reduction of mean free path (λ), moves

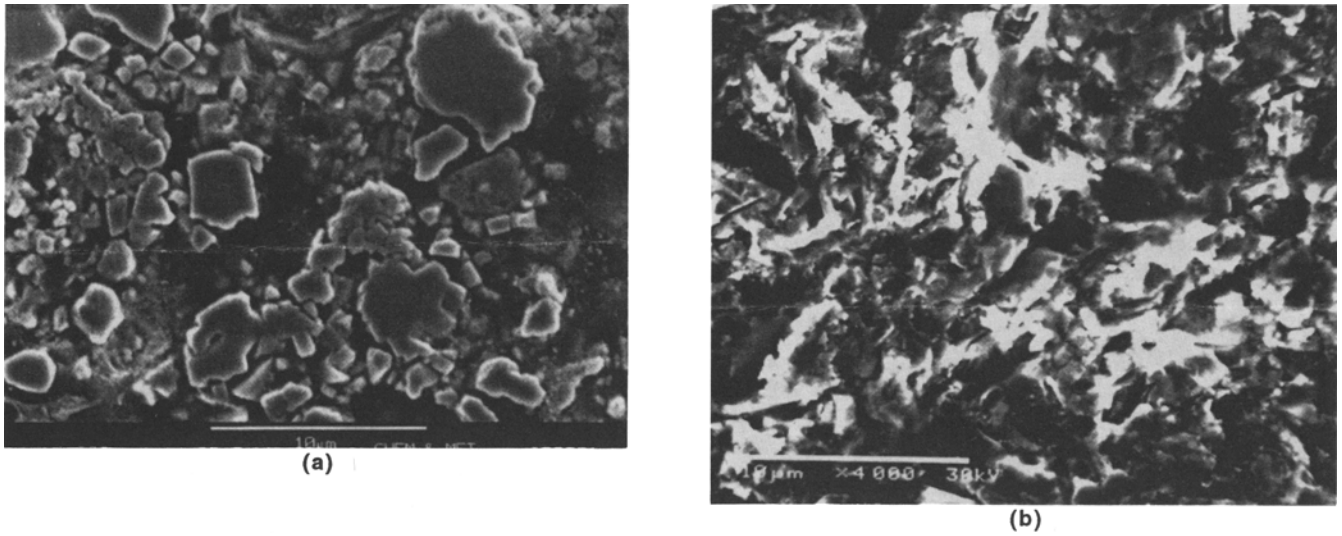

Figure 4 (a) WC-17 wt% Co, APS as polished prior to testing and (b) WC-17wt% Co, APS after erosion test.

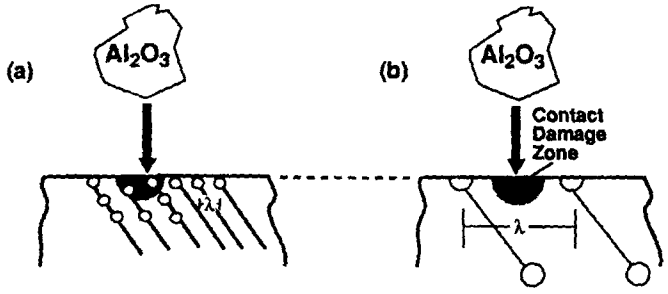

Figure 5 Schematic representation of erosion damage zone and relation to mean free path (λ) between WC grains. The symbol "O" represents WC grains.

sintered material toward higher erosion resistance. It is noteworthy that in the prior study,[19] erosion resistance increased in a nonlinear fashion as λ approached zero. The much higher erosion resistance of sintered WC-12 wt% Co can be attributed to a number of factors: (1) the significantly lower value of λ compared to all other materials in this study and (2) recrystallization and grain growth during sintering. The test methodology used herein may have also played a role insofar as the coating erosion test duration was limited by the time required to reach the substrate (typically 30 s), whereas prior tests[19] with sintered materials lasted 3 min.

Figure 4 compares scanning electron microscopy (SEM) micrographs of the surface of the polished (as-sprayed) and eroded surfaces of the WC-17 wt% Co APS coatings. It is clear from the polished surface micrograph (Fig. 4a) that there is considerable segregation of carbides in the APS coating. The eroded APS surface in Fig. 4(b) shows large deformed areas and indications of plastic deformation and fracture. The lack of WC microstructural features indicates the ease of removal of both WC and cobalt-rich binder. It is clear that variations in microstructure can lead to increased erosion resistance; however, with 17 wt% cobalt content, only small improvements can be expected—up to the level of the WC-17 wt% Co sintered material (Fig. 2b).

Figure 5 is a schematic representation of how an eroding Al_2O_3 particle interacts with microstructures that correspond to lower (Fig. 5a) and higher (Fig. 5b) cobalt contents. The shaded region indicates a singular contact damage zone that involves both WC and metal binder (Fig. 5a), whereas Fig. 5(b) shows the possibility of isolated erosion of binder, leading to easy removal of the wear-resistant WC grains. An important microstructural factor influencing erosion is the mean free path of the binder. The sintered WC-12 wt% Co material, in general, has a lower mean free path compared to that of sintered WC-17 wt% Co, which translates into better erosion resistance. Although this is also applicable to plasma-sprayed coatings, porosity, intersplat strength, and carbide/matrix bond strength become overriding factors in determining erosion resistance. Rangaswamy[6] has studied the erosion properties of plasma-sprayed WC-Co coatings with a 45 and 90° impingement angle. He concluded that macroporosity and microporosity played a significant role in lowering the erosion resistance of the coating. More recently, Mehan and Rairden[23] demonstrated this effect by plotting the erosion rate as a function of volume porosity for several WC-Co thermally sprayed coatings and were able to obtain a continuous curve of erosion rate with porosity. Another noteworthy microstructural effect is that the APS and HVOF coatings, even with large cobalt pools, display good resistance to erosion. Carbon loss and carbide decomposition effectively increase the mean free path of the binder. Both APS and HVOF coatings show higher mean free path than the VPS and sintered materials. The dissolution of W and C in the matrix causes substantial increase

in the hardness of the matrix and may compensate for the decreased carbide content in APS and HVOF coatings.

In the previous study on sintered WC-Co materials,[19] it was shown that the abrasion and erosion characteristics were correlated to hardness, fracture toughness, and volume fraction of cobalt. These samples were homogeneous with no porosity and strictly WC and Co phases in the microstructure. In the thermally sprayed coatings, additional differences arise due to porosity, lamellar structure, and metastable phases such as W_2C, W, and Co_xW_xC compounds. Although hardness and fracture toughness measurements take into account some of these differences, it is anticipated that this can explain some of the minor discrepancies in the correlation in this study. This is an area for further investigation.

5. Conclusions

The microstructure, mechanical properties, and wear resistance of thermally sprayed and sintered WC-Co materials were examined. The study has shown that the wear resistance of thermally sprayed WC-12wt% Co and WC-17wt% Co materials to diamond abrasion is not strongly affected by the cobalt content, whereas the wear resistance to gas jet Al_2O_3 particle erosion is more prominently controlled by the cobalt content. The abrasive and erosive wear resistance of thermally sprayed WC-Co is dependent on porosity, mean free path of binder, and carbide grain size. The wear results obtained in this study can be understood on the basis of mechanical properties and microstructure. For coatings, a porous structure causes poor intersplat bond, which, in turn, lowers the hardness and fracture toughness. It has also been shown that a derived mechanical property/microstructure parameter can be used in most cases to describe abrasive and erosive wear resistance of thermally sprayed and sintered WC-Co materials as follows:

$$\text{Wear resistance} \quad \alpha \left(K_{IC}^{3/8} H^{1/2}\right)\left(\frac{V_f^{Co}}{1 - V_f^{Co}}\right)$$

This relationship provides a means for assessing wear resistance of WC-Co coatings intended for industrial applications requiring abrasion and erosion resistance. This further suggests that coating selection and specification should be based on fundamental properties of the deposit rather than on a process or composition-based methodology.

The influence of anisotropic physical properties, particularly fracture toughness, in thermally sprayed WC-Co coatings is of significance and should be further investigated with regard to coating quality control and performance.

Acknowledgments

The authors thank Glenn Bancke and Professor Herbert Herman of the State University of New York at Stony Brook for their assistance in plasma spraying of the specimens. We are also grateful to Dr. David Houck and Vidhu Anand of GTE for their critical review of the manuscript and to Kathy Hammerly, Jack Vanderpool, and Dave Estelle, also of GTE, for their help. The experimental measurements performed by John Luongo and Peter Ness of GTE Laboratories are sincerely appreciated. The support provided by the Technical Publications Department at GTE Laboratories is also gratefully acknowledged.

References

1. J. Gurland, The Fracture Strength of Sintered Tungsten Carbide-Cobalt Alloys in Relation to Composition and Particle Spacing, *Trans. AIME*, Vol 227, 1963, p 1146-1150.
2. H.E. Exner and J. Gurland, A Review of Parameters Influencing Some Mechanical Properties of Tungsten Carbide-Cobalt Alloys, *Powder Metall.*, Vol 13 (No. 25), 1970, p 13-30.
3. R.A. Cutler and A.V. Virkar, The Effect of Binder Thickness and Residual Stresses on the Fracture Toughness of Cemented Carbides, *J. Mater. Sci.*, Vol 20, 1985, p 3557-3573.
4. J. Nerz, B. Kushner, and A. Rotolico, Effects of Deposition Methods on the Physical Properties of Tungsten Carbide-12 wt.% Cobalt Thermal Spray Coatings, in *Protective Coatings: Processing and Characterization*, R.M. Yazici, Ed., The Minerals, Metals & Materials Society, 1990, p 135-143.
5. T.A. Mantyla, K.J. Niemi, P.M.J. Vuoristo, G. Barbezat, and A.R. Nicoll, Abrasion Wear Resistance of Tungsten Carbide Coatings Prepared by Various Thermal Spraying Techniques, in *2nd Plasma-Technik Symposium*, Vol 1, S.B. Sandmeier, P. Huber, H. Eschnauer, and A. Nicoll, Ed., Lucerne/Switzerland, 1991, p 287-297.
6. S. Rangaswamy, "Metallurgical Characterization of Plasma Sprayed WC-Co Coatings," Ph.D. thesis, State University of New York, Stony Brook, 1987.
7. V. Ramnath and N. Jayaraman, Characterization and Wear Performance of Plasma Sprayed WC-Co Coatings, *Mater. Sci. Technol.*, Vol 5 (No. 4), 1989, p 382-388.
8. M.E. Vinayo, F. Kassabji, J. Guyonnet, and P. Fauchais, Plasma Sprayed WC-Co Coatings: Influence of Spray Conditions (Atmospheric and Low Pressure Plasma Spraying) on the Crystal Structure, Porosity, and Hardness, *J. Vac. Sci. Technol. A*, Vol 3 (No. 6), 1985, p 2483-2489.
9. D. Tu, S. Chang, C. Chao, and C. Lin, Tungsten Carbide Phase Transformation During the Plasma Spray Process, *J. Vac. Sci. Technol. A*, Vol 3 (No. 6), 1985, p 2479-2482.
10. O.V. Roman, A. Ilyuschenko, A. Verstak, and M. Nekrashevich, Evaluation of Wear Resistance of APS and VPS Metal Carbide/Metal Coating Systems, in *Proc. 1st Plasma-Technik-Symposium*, Vol 2, S.B. Sandmeier, P. Huber, H. Eschnauer, and A. Nicoll, Ed., Lucerne/Switzerland, 1988, p 15-23.
11. B. Schultrich, L.-M. Berger, J. Henke, and A. Oswald, Influence of Carbide Powder Composition on Decarburization During Air Plasma Spraying, in *Proc. 2nd Plasma-Technik-Symposium*, Vol 2, S.B. Sandmeier, P. Huber, H. Eschnauer, and A. Nicoll, Ed., Lucerne/Switzerland, 1991, p 363-370.
12. S. Rangaswamy and H. Herman, Metallurgical Characterization of Plasma Sprayed WC-Co Coatings, in *Advances in Thermal Spraying*, Pergamon Press, 1986, p 101-110.
13. M.R. Dorfman, B.A. Kushner, J. Nerz, and A.J. Rotolico, A Technical Assessment of High Velocity Oxygen-Fuel Versus High Energy Plasma Tungsten Carbide Coatings for Wear Resistance, in *Proc. 12th Int. Thermal Spray Conference*, I.A Bucklow, Ed., The Welding Institute, London, 1989, p 108.
14. K.V. Rao, D.A. Somerville, and D.A. Lee, Properties and Characterization of Coatings Made Using Jet Kote Thermal Spray Process, in *Advances in Thermal Spraying*, Pergamon Press, 1986, p 873-882.
15. Y. Arata, A. Ohmori, and E. Gofuku, WC-Co High Energy Thermal Sprayed Coatings, *Trans. Jpn. Weld. Res. Inst.*, Vol 14 (No. 2), 1985, p 267-273.

16. S. Basinska-Pampuch and T. Gibas, Observations on Some Plasma-Sprayed Metal Carbides, *Ceram. Int.*, Vol 3 (No. 4), 1977, p 152-158.
17. E.A. Almond, L.A. Lay, and M.G. Gee, Comparison of Sliding and Abrasive Wear Mechanisms in Ceramics and Cemented Carbides, *Inst. Phys. Conf. Ser. No. 75: Science of Hard Materials*, Adam Hilger, Chapt 9, 1986, p 919-948.
18. J.G. Baldoni, S.F. Wayne, and S.-T. Buljan, Cutting Tool Materials: Mechanical Properties Wear-Resistance Relationships, *American Society for Lubrication Engineers Trans.*, Vol 29 (No. 3), 1986, p 347-352.
19. S.F. Wayne, J.G. Baldoni, and S.-T. Buljan, Abrasion and Erosion of WC-Co with Controlled Microstructures, *Tribology Trans.*, Vol 33 (No. 4), 1990, p 611-617.
20. A.G. Evans and E.A. Charles, Fracture Toughness Determination by Indentation, *J. Am. Ceram. Soc.*, Vol 59 (No. 7-8), 1976, p 371-372.
21. H. Nakahira, K. Tani, K. Miyakima, and Y. Harada, Anisotropy of Thermally Sprayed Coatings, in *Proc. Int. Thermal Spray Conf.*, C.C. Berndt, Ed., ASM International, 1992, p 1011.
22. S. Sampath and H. Herman, Microstructure of Vacuum Plasma Sprayed Coatings, in *Proc. Nat. Thermal Spray Conf.*, D.L. Houck, Ed., ASM International, 1988, p 1.
23. R.L. Mehan and J.R. Rairden, "Improved Materials for Durable Rings, Liners, and Injector Nozzles," Topical Report, Dept. of Energy (DOE/MC/23174-2913), June 1990.